Antibacterial Agent Discovery Using Thymidylate Synthase Biolibrary Screening

M. Paola Costi,*,† Arianna Gelain,‡ Daniela Barlocco,‡ Stefano Ghelli,§ Fabrizia Soragni,† Fabiano Reniero,# Tiziana Rossi,|| Antonio Ruberto,|| Claude Guillou,|| Antonio Cavazzuti,† Chiara Casolari,⊥ and Stefania Ferrari†

Dipartimento di Scienze Farmaceutiche, Università degli Studi di Modena e Reggio Emilia (UNIMORE), Via Campi 183, 41100 Modena, Italy, Istituto di Chimica Farmaceutica e Tossicologica, Università degli Studi di Milano, Viale Abruzzi 42, 20131 Milano, Italy, Spinlab S.r.l., Via Tamagno 3, 42048 Rubiera (RE), Italy, Physical and Chemical Exposure Unit, Institute for Health and Consumer Protection, European Commission Joint Research Centre, 21020 Ispra (VA), Italy, Dipartimento di Scienze Biomediche, Sezione di Farmacologia, Università degli Studi di Modena e Reggio Emilia, Via Campi 287, 41100 Modena, Italy, and Dipartimento di Medicina di Laboratorio, Università degli Studi di Modena e Reggio Emilia, Via del Pozzo 71, 41100 Modena, Italy

Received November 23, 2005

Thymidylate synthase (TS, ThyA) catalyzes the reductive methylation of 2′-deoxyuridine 5′-monophosphate to 2′-deoxythymidine 5′-monophosphate, an essential precursor for DNA synthesis. A specific inhibition of this enzyme induces bacterial cell death. As a second round lead optimization design, new 1,2-naphthalein derivatives have been synthesized and tested against a TS-based biolibrary, including human thymidylate synthase (hTS). Docking studies have been performed to rationalize the experimentally observed affinity profiles of 1,2-naphthalein compounds toward *Lactobacillus casei* TS and hTS. The best TS inhibitors have been tested against a number of clinical isolates of Gram-positive-resistant bacterial strains. Compound 3,3-bis(3,5-dibromo-4-hydroxyphenyl)-1*H*,3*H*-naphtho[1,2-*c*]furan-1-one (**5**) showed significant antibacterial activity, no in vitro toxicity, and dose-response effects against *Staphylococcus epidermidis* (MIC = 0.5−2.5 μg/mL) clinical isolate strains, which are resistant to at least 17 of the best known antibacterial agents, including vancomycin. So far this compound can be regarded as a leading antibacterial agent.

Introduction

Thymidylate synthase (TS, ThyA) (E.C. 2.1.1.45) is a key enzyme in DNA synthesis. It catalyzes the reductive methylation of 2′-deoxyuridine 5′-monophosphate (dUMP) to 2′-deoxythymidine 5′-monophosphate (dTMP), which, as a triphosphate, is a substrate of DNA polymerase and is incorporated into the DNA. The catalyzed reaction is assisted by N^5,N^{10}-methylenetetrahydrofolate (mTHF), which acts as both a monocarbon unit donor and reducing agent[1] (Figure 1). TS inhibition leads to thymineless death, which is a complex mechanism affecting the replication process. Therefore, TS has been regarded as a target for anticancer drugs.[2] The enzyme has also been implicated in the protein synthesis regulation pathway[3,4] and apoptotic process,[4] as well as in the development of Alzheimer's disease.[5] It has also been regarded as a potential target for antibacterial and antifungal chemotherapy.

TS is inhibited by substrate analogues, such as 5-fluoro-2′-deoxyuridine 5′-monophosphate (FdUMP), or cofactor analogues, such as ZD1694 and pemetrexed (Alimta) (Chart 1). Recently, nonclassical anti-folate inhibitors (NCAI) that are able to specifically inhibit the microbial enzyme with respect to human thymidylate synthase (hTS)[6−14] have been reported, among them 3,3-bis(3-chloro-4-hydroxyphenyl)-1*H*,3*H*-naphtho-[1,8-*c*,*d*]pyran-1-one (α**156**, compound **10** in this paper) and didansyltyrosine (DDT)[7,9,12−14] (Chart 1). In particular, compound **10** proved to specifically bind *Lactobacillus casei* TS (LcTS) with submicromolar inhibition constant (K_i = 0.7 μM) and was 30-fold more specific with respect to hTS.[14] This compound also showed antimicrobial activity against Gram-positive bacteria, with a minimum inhibitory concentration (MIC) of 1.8 μg/mL.[13]

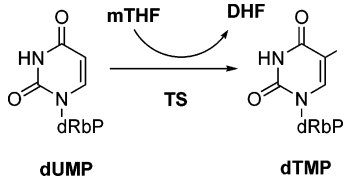

Figure 1. TS catalytic reaction (dRbP = 2′-dexyribose-5′-monophosphate).

Detailed studies on protein−ligand interaction, such as X-ray three-dimensional structure determination, site-directed mutagenesis experiments, and computational studies,[14,15] have demonstrated that these molecules show a multiple binding mode, raising the important issue of the reliability of a structure-based drug design approach. In a recent study,[15] it was proposed that the basis for species specificity of the naphthalein inhibitors lies in the different flexibility of the human enzyme compared to bacterial ones. The bacterial enzymes, such as LcTS, can accommodate the naphthalein derivative (**10**) in its binding site close to the small domain, a specific sequence (70 residues) that enlarges the active site domain.[14,16] By contrast, in human enzyme the corresponding binding site is partially inaccessible. As a consequence, inhibitor **10** cannot bind to its preferred site in hTS and the affinity for this enzyme decreases, thus ameliorating the specificity index ($K_{i\ hTS}$/ $K_{i\ LcTS}$).[15]

In an attempt to enhance the affinity and specificity of the naphthalein series, new 1,2-naphthalein derivatives (**1**−**8**, Chart 2) were designed and synthesized along with two new 1,8-naphthalein derivatives (**16**, **18**, Chart 2). All the compounds and eight previously synthesized 1,8-naphthalein derivatives (**9**−**15**, **17**)[9,13,14] (Chart 2), selected among the closest analogues

* To whom correspondence should be addressed. Phone: 0039-059-205-5134. Fax: 0039-059-205-5131. E-mail: costimp@unimore.it.
† Dipartimento di Scienze Farmaceutiche, Università degli Studi di Modena e Reggio Emilia.
‡ Università degli Studi di Milano.
§ Spinlab S.r.l.
# Institute for Health and Consumer Protection.
|| Dipartimento di Scienze Biomediche, Università degli Studi di Modena e Reggio Emilia.
⊥ Dipartimento di Medicina di Laboratorio, Università degli Studi di Modena e Reggio Emilia.

10.1021/jm051187d CCC: $33.50
Published on Web 09/07/2006

Chart 1

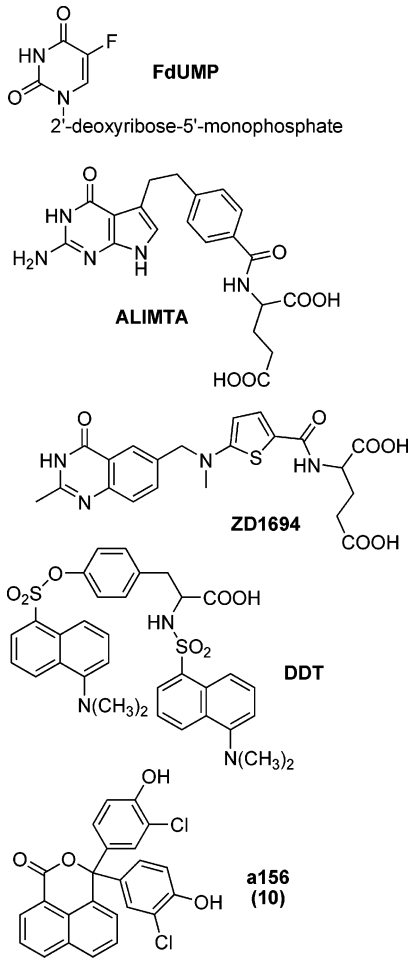

that were most potent in preliminary assays, were tested against a TS-based biolibrary containing the following enzymes: *Lactobacillus casei* (LcTS), *Escherichia coli* TS (EcTS), *Cryptococcus neoformans* TS (CnTS), human TS (hTS), and human dihydrofolate reductase (hDHFR). To rationalize the observed affinity profiles of this new series, a modeling study was performed and the interactions of compounds **1** and **2** with LcTS and hTS were explored using the AutoDock 3.0.5 program. Moreover, several molecules with significant affinity (**5**, **8**, **10**, **13**−**16**, **18**) were tested against wild-type bacterial strains. In addition, the most active compounds were screened against clinical isolate resistant bacterial strains and their cytotoxicity was evaluated against VERO cells.

Design and Synthesis

The design of the new compounds was based on the known X-ray crystal structure of the binary complex LcTS−phenolphthalein (pth) (Figure 2).[17] Since the 1,2-naphthalein derivatives may exist in two isomeric forms, namely, the α-isomers (**1**, **3**−**6**) and the *β*-isomers (**2**, **7**, **8**), both structures were considered. Assuming that 1,2-naphthaleins have the same binding mode as pth, the benzene ring added to the phthalein core in the α-isomer derivatives would be directed toward the folate binding site and would interact with I81, E84, and V314, whereas in the *β*-isomer derivatives the benzene ring is directed toward the small domain region and interacts with E84, W85, F104, and V316. Although we hypothesized that increasing the aromatic bulk with an additional benzene ring could be critical for pth-derived molecules, the matching of **1** and **2** with pth

Chart 2

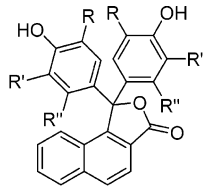

	R	R'	R"
1	H	H	H
3	I	H	H
4	Br	H	H
5	Br	Br	H
6	$CH(CH_3)_2$	H	CH_3

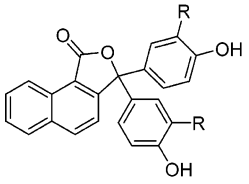

	R
2	H
7	Cl
8	F

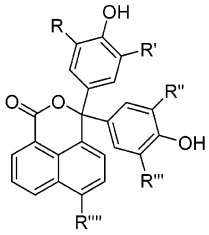

	R	R'	R"	R'''	R''''
9	I	H	I	H	H
10	Cl	H	Cl	H	H
11	Cl	H	Cl	H	Cl
12	Cl	Cl	Cl	Cl	H
13	Br	H	H	H	H
14	Br	H	Br	H	H
15	Br	Br	Br	Br	H
16	Br	H	Br	H	Cl
17	F	H	F	H	H
18	F	H	F	H	Cl

shows that these compounds could be allocated to the same binding site without visible impediment to good fitting. On these bases, halogen substituents have also been introduced into this new series to possibly enhance their inhibitory activity and specificity, as seen in the previously reported 1,8- and 2,3-naphthalein derivatives.[9,13,14]

1,2-Naphthalic anhydride (**I**) was synthesized according to a previously reported method.[18] Its condensation with phenol under Friedel−Crafts conditions gave the 3,3-bis(4-hydroxyphenyl)-1*H*,3H-naphtho[1,2-*c*]furan-1-one (**1**) as the main reaction product, together with its isomer **2** at a very low concentration. The iodo (**3**) and bromo (**4**, **5**) derivatives were obtained from **1** by treatment with iodine, chloride, or bromine, respec-

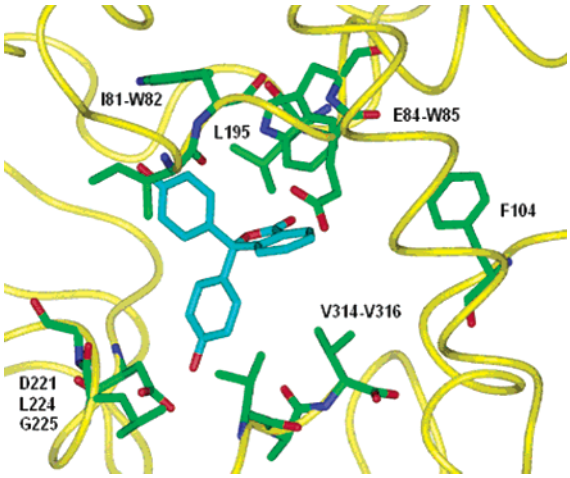

Figure 2. Detail of the X-ray crystal structure of the binary complex LcTS−pth.

Scheme 1[a]

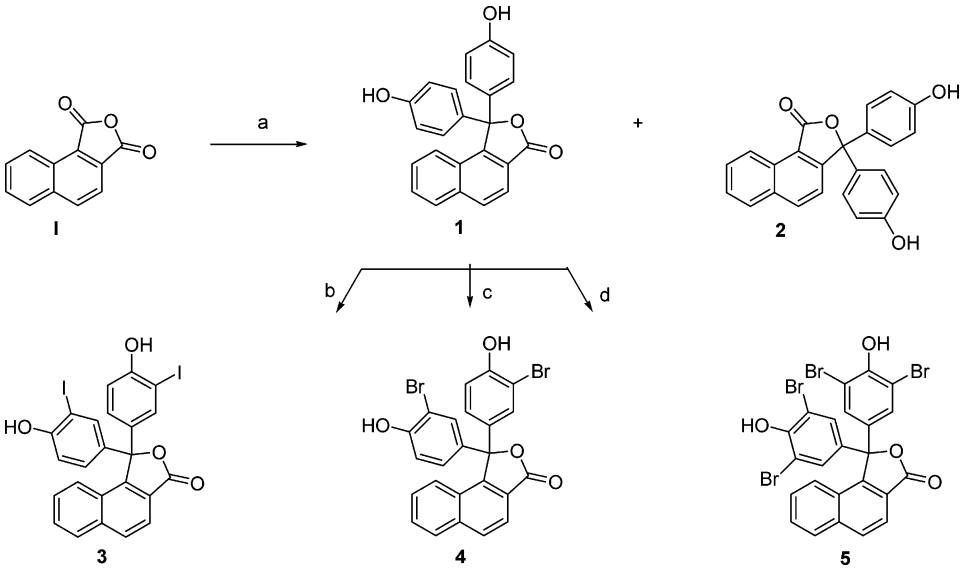

[a] (a) phenol, $SnCl_4$, Δ; (b) ICl, CH_3COOH, room temp; (c) Br_2, CH_2Cl_2, room temp; (d) Br_2, CH_3COOH, room temp.

Scheme 2[a]

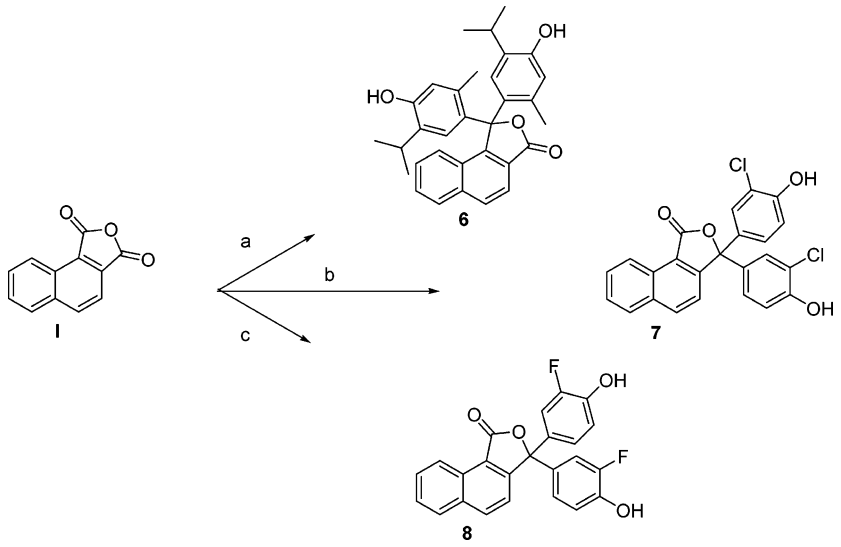

[a] (a) thymol, $AlCl_3$, Δ; (b) *o*-chlorophenol, H_2SO_4, Δ; (c) *o*-fluorophenol, H_2SO_4.

tively (Scheme 1). Compounds **6**−**8** were prepared from the 1,2-naphthalic anhydride (**I**) by heating with the appropriate substituted 2-phenol in the presence of aluminum trichloride (Scheme 2). It should be noted that while in the case of **6** only the α-isomer was obtained, the opposite was true for **7** and **8**, which were collected in the *β*-form.

Compounds **16** and **18** were synthesized according to a previously reported method.[13]

Profiling Enzyme Inhibition

A TS-based biolibrary was designed to determine a biological affinity profile and to provide information on the species specificity and selectivity of the synthesized compounds. In particular, the issue of specificity was addressed, including a number of TS from pathogenic organisms in the biolibrary, such as LcTS, EcTS, CnTS, in addition to hTS. Selectivity was verified toward the hDHFR enzyme, a typical TS metabolically related enzyme that works in competition with hTS in the binding of many classic folate analogues, such as CB3717 (10-propargyl-5,8-dideazafolic acid) and methotrexate (MTX). The apparent inhibition constant (K_i) values of the tested compounds were determined, and the specificity (SI) and selectivity indices (SSI) were calculated. The results are shown in Table 1 and Figure 3.

In the 1,2-naphthalein series, all the compounds, with the exception of **6**, inhibited the pathogen TS. Their K_i values were 1.4−11 μM against LcTS, 0.3−8.5 μM against EcTS, and 0.4−13 μM against CnTS. In particular, **2** and **8** were the most active compounds against LcTS with a K_i of 1.4 μM. Compound **2** also showed the lowest K_i (0.3 μM) against EcTS, while **1** was the most potent against CnTS (K_i = 0.4 μM). 1,2-Naphthalein compounds generally inhibited hDHFR at a higher level than hTS (K_i in the range 3.9−110 μM vs >100 μM), with the sole exception of **2** (K_i of 35 μM vs 0.4 μM). Compound **7** was equipotent against the two enzymes (K_i of 35 and 34 μM, respectively).

In the 1,8-naphthalein series, K_i values of 0.7−31 μM vs LcTS, 0.4 μM to 11 mM vs EcTS, and 3.3−35 μM vs CnTS were observed. The most active compounds were **10** and **11** against LcTS (K_i = 0.7 μM), **13** against EcTS (K_i = 0.4 μM),

Table 1. Inhibition Constants (K_i), Specificity Index (SI = $K_{i\ hTS}/K_{i\ enzyme}$) and Selectivity Index (SSI = $K_{i\ hDHFR}/K_{i\ hTS}$) for Compounds **1**−**18** against LcTS, EcTS, CnTS, hTS, and HDHFR

	K_i (μM)					SI			SSI
	LcTS	EcTS	CnTS	hTS	hDHFR	LcTS vs hTS	EcTS vs hTS	CnTS vs hTS	hTS vs hDHFR
1	11	4.4	0.4	≫132[a]	110	≫12	≫30	≫330	≪1
2	1.4	0.3	0.6	0.4	35	0.3	1	1	88
3	2.0	1.5	4.5	≫245[a]	3.9	≫123	≫163	≫54	≪0.01
4	6.6	0.9	2.7	≫132[a]	33	≫20	≫147	≫49	≪0.2
5	1.7[b]	8.5[b]	13	≫245[a]	69	≫144	≫29	≫19	≪0.3
6	ND[c]	ND[c]	ND[c]	ND[c]	13				
7	3.9	1.2	8.1	34	35	9	28	4	1
8	1.4	1.4	3.5	≫132[a]	109	≫94	≫94	≫38	≪1
9	31		16	≫132[a]	94	≫4		≫8	≪1
10	0.7[b]	0.6[b]	35	30[b]	5.2	43	50	1	0.2
11	0.7[b]	13	9.6	≫120[a]		≫171	≫9	≫13	
12	2	5.3	3.3	5.7	28	3	1	2	5
13	1	0.4	5.2	≫132[a]	3.4	≫132	≫330	≫25	≪0.02
14	6.8	0.9	13	4.7	15	1	5	0.4	3
15	0.9	≫11 mM[a]	4	3.2	9.5	4	≫0.0003	1	3
16	0.8[c]	4.1[c]	4.1	≫245[a]	13	≫306	≫60	≫60	≪0.05
17	1.6[b]	1.1[b]	6.4	≫402[a]	42	≫251	≫365	≫63	≪0.1
18	1.8[b]	1.1[b]	6.5	≫245[a]	12	≫136	≫223	≫38	≪0.05
CB3717	0.06[b]	0.06[b]		0.03[b]		1	1		

[a] Calculated supposing 2% inhibition at the maximum solubility concentration (24 μM for **11**; 27 μM for **1**, **4**, **8**, **9**, **13**; 50 μM for **3**, **5**, **16**, **18**; 82 μM for **17**; 2.2 mM for **15**). [b] Already reported.[9,13−15] [c] Not detectable because of the insolubility of the compound (solubility less than 10 μM).

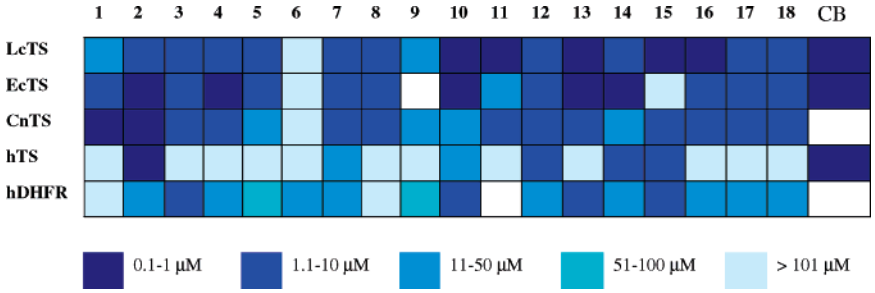

Figure 3. Grid of affinity profiling. K_i ranges are described by color code.

and **12** against CnTS (K_i = 3.3 μM). In addition, better activity toward hDHFR versus hTS (K_i = 3.4−94 μM) was found in this series. Only three compounds were more active against hTS than hDHFR, namely, **12** (K_i of 28 vs 5.7 μM), **14** (K_i of 25 vs 4.7 μM), and **15** (K_i of 9.5 vs 3.2 μM).

In both series, all the compounds were competitive inhibitors of the enzymes with respect to the folate cofactor.

When specificity was considered in both series, 12 out of 18 compounds were 1 order of magnitude more specific for LcTS than hTS (SI = 9−306). In particular, compounds **3**, **5**, **8**, **11**, **13**, and **16**−**18** were at least 100-fold more active against LcTS with respect to hTS (SI = 94−306), **16** being the best representative. The same 12 compounds were also more active against EcTS than hTS (SI = 9−365). Compounds **3**, **4**, **8**, **13**, and **16**−**18** show a specificity index greater than or around 100, the best being **17**. Finally, 10 compounds (**1**, **3**−**5**, **8**, **11**, **13**, and **16**−**18**) were specific for CnTS vs hTS, with a specificity index of 13−330, compound **1** having the highest value.

However, when selectivity between hTS and hDHFR was considered, only compound **2** showed a significant index (SSI = 88), all the other derivatives being either inactive toward hTS or equipotent against the two enzymes.

It is important to note that any new compound to be considered as a potential antibacterial should not be active against hDHFR. Unfortunately, in our case the compounds with specific affinity vs LcTS and EcTS (**13**, **16**−**18**) with respect to hTS also showed measurable activity against hDHFR.

Altogether, 1,2- and 1,8-naphthalein derivatives showed some similarity in their enzyme inhibition profile. In particular, both series were species-specific against EcTS with respect to hTS. By contrast, 1,8-naphthalein derivatives were species-specific against LcTS whereas 1,2-naphthalein compounds were species-specific against CnTS with respect to hTS. Finally, the latter compounds were less active against hDHFR than 1,8-naphthalein derivatives.

Modeling

The three-dimensional models of compounds **1** and **2** were built using InsightII and then docked in the active site of the three-dimensional crystallographic structure of LcTS and hTS in the presence of a dUMP molecule, using the AutoDock 3.0.5 program.

Thirty-seven distinct conformational clusters, out of 100 runs, were obtained for compounds **1** and **2** docked against LcTS. In the case of hTS, 26 and 24 distinct conformational clusters, out of 50 runs, were obtained for compounds **1** and **2**, respectively. The difference in the calculated docked energy among these clusters were around 2 kcal/mol in the case of LcTS and 3.5 and 2.4 kcal/mol in the case of hTS, for **1** and **2**, respectively. These compounds are characterized by a pseudo-3-fold symmetry through which they can change their orientations without changing their patterns of interactions; therefore, even if the program considered all these clusters as distinct, these binding conformations can be grouped as multiple orientations for the two main binding sites previously identified:[14,15] the folate-binding site and the crystallographic binding site of compound **10** (near the small domain). The three-dimensional crystallographic structure of the complex LcTS−**10**[14] showed that this compound binds 5 Å away from the folate binding site in a less conserved region of the enzyme and interacts with many

Table 2. Docking Results for Compounds **1** and **2** to LcTS and HTS Using AutoDock 3.0.5, Showing Percentage of Ligand Conformations Predicted at the Specified Site (a) and Estimated Free Energy of Binding (kcal/mol) of the Best-Scored Conformation at the Specified Site (b)

	LcTS				hTS			
	folate		small domain		folate		small domain	
compd	a	b	a	b	a	b	a	b
1	50	−3.14	40	−1.99	50	−3.31	32	−1.88
2	58	−3.52	41	−2.46	62	−3.10	26	−1.89

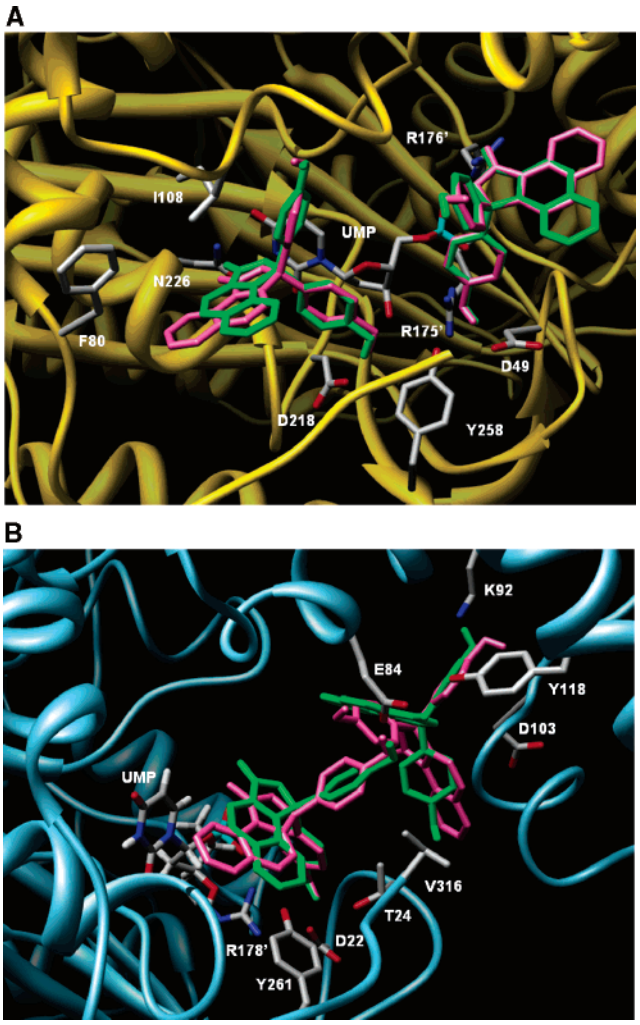

Figure 4. Low-energy binding modes of compounds **1** (green) and **2** (pink) in hTS (A) and LcTS (B). In each enzyme, two possible binding modes are shown: in the folate binding site (on the right of the images) and in the binding site near the small domain (on the left of the images). Only the most important residues (colored by atom) interacting with ligands are shown.

residues of the small domain. All the conformations that were outside the active site were disregarded.

The results suggest that these molecules can bind in these two regions with multiple binding modes in both enzymes. The folate-binding site is calculated to be more occupied and energetically more favorable than the second (by about 1−1.4 kcal/mol) (Table 2).

The most favorable binding modes in each site of both enzymes can be described in detail for compounds **1** and **2** (Figure 4) as follows.

Compound **1** binds in the folate-binding site of hTS, forming hydrogen bonds through its phenol hydroxyls with the side chain of D218, the carboxyl function of I108, and the hydroxyl group in the 3′ position of the ribose of dUMP and through its carbonyl function with the side chain amide of N226. It also interacts through van der Waals interactions with other seven residues, including M311.

A second binding site for compound **1**, nearer the small domain region, was also predicted in hTS. In this binding site, compound **1** forms hydrogen bonds through its carbonyl function with the imino group of R176′ and through its phenol hydroxyls with the carboxyl function of D49, the hydroxyl of Y258, and the imino group of R175′. It also forms van der Waals interactions with other eight seridues, including T51 and V313.

Compound **2** binds to hTS in a similar manner. In the folate-binding site, it forms hydrogen bonds with D218 and I108, N226, and the hydroxyl group in the 3′ position of the ribose of dUMP and interacts through van der Waals interactions with V79, F80, W109, N112, L221, G222, F225, and Y258 through its phenols and naphthalene rings. The main difference with respect to compound **1** is that compound **2**, through its terminal naphthalene ring, does not interact with M311 but with V79 and F80.

Compound **2** also binds in a second binding site of hTS, near the small domain. It forms hydrogen bonds with R176′, D49, Y258, and R175′ and van der Waals interactions with R50, N112, F117, L192, M311, and A312. There is only a slight difference in the interaction pattern with respect to compound **1** because of the change in the pose of the terminal naphthalene ring. In the case of compound **1** the terminal naphthalene ring interacts with T51 and V313, whereas in the case of compound **2** the terminal naphthalene ring interacts with R50. However, apart from these differential interactions, this part of the molecule is exposed to the solvent (Figure 4).

Regarding LcTS, in the folate-binding site, compound **1** interacts with D22, T24, E84, Y261, and R178′ by forming hydrogen bonds through its phenol hydroxyls and with R23, L195, D221, L224, V314, A315, and V316 through van der Waals interactions.

In the second binding site of LcTS, near the small domain, compound **1** forms hydrogen bonds with the side chain amino group of K92, with the nitrogen of the D103 backbone, with the C-terminus carboxyl group of V316 through its phenol hydroxyls, and with the hydroxyl of Y118 and the backbone nitrogen of G105 through its lactonic function. It also forms van del Waals interactions with R23, T24, E84, E88, M101, T1021, F104, H106, and A194.

Compound **2** shows, in the folate-binding site of LcTS, the same binding mode as compound **1**, but it also interacts with G225.

On the other hand, in the second binding site of LcTS, which is near the small domain, compound **2** shows a different binding mode with respect to compound **1** even though it interacts with the same residues. It forms hydrogen bonds through its phenyl hydroxyl with the side chains of K92 and E84 and the backbone carbonyl of M101.

In agreement with experimental inhibition activity data against LcTS, AutoDock predicts similar behavior in enzyme binding for both compounds. On the other hand, on the basis of inhibition activity data against hTS, one could expect that some differences may be found in binding to hTS. However, the only difference between the most favorable binding modes of compounds **1** and **2** in the hTS′ active site is that the terminal naphthalene ring of compound **2**, in its interaction with the folate binding site, does not interact with M311 but with V79 and F80. In particular, F80 may change its conformation and form a stacking interaction with the naphthalene ring of the ligand.

Table 3. MIC for Compounds **5**, **8**, **10**, **13**−**16**, **18** (μg/mL)

	compd								
strains	**5**	**8**	**10**	**13**	**14**	**15**	**16**	**18**	cpx
Enterococcus faecalis ATCCC29212	2.5	25	10	25	10	5	5	25	12.5
Escherichia coli 256	>25	>50	>25	>50	>50	>50	>25	>50	>25
Escherichia coli 292	>25	>50	>25	>50	>50	>50	>25	>50	>25
Listeria monocytogenes 3	2.5	25	2.5	10	2.5	2.5	5	10	2.5
Listeria monocytogenes 4	2.5	25	10	10	5	2.5	2.5	10	1
Listeria monocytogenes 5	2.5	25	5	10	5	2.5	5	10	2.5
Listeria monocytogenes 6	2.5	25	10	10	5	2.5	2.5	10	2.5
Listeria monocytogenes 7	2.5	25	5	10	1	5	2.5	10	1
Listeria monocytogenes 8	2.5	25	5	25	5	5	5	25	1
Listeria monocytogenes ATCC4428	2.5	25	5	10	5	2.5	1	10	2.5
Staphylococcus aureus 341	2.5	25	5	25	5	2.5	2.5	10	1.2
Staphylococcus aureus 343	2.5	25	5	10	5	2.5	1	10	0.5
Staphylococcus aureus K28	2.5	25	>25	25	5	5	2.5	10	0.5
Staphylococcus aureus ATCC29213	2.5	25	5	10	5	2.5	2.5	10	0.5
Staphylococcus haemolyticus ATCC2997	2.5	25	2.5	10	5	5	5	10	2.5
Staphylococcus saprophiticus ATCC15305	1	25	2.5	10	5	2.5	1	10	1
Citrobacter 224	>25	>50	>25	>50	>50	>50	>25	>50	>25
Streptococcus 42	2.5	25	5	10	5	5	1	10	>5

This would be an important specific interaction with hTS that could contribute significantly to the good affinity and inhibition activity of compound **2** for hTS with respect to compound **1** (K_i vs hTS of 0.4 and $\gg$132 μM for compounds **2** and **1**, respectively). Moreover, a deeper analysis of all the predicted binding modes for each compound reveals that there are few secondary binding modes predicted by AutoDock for compound **2** that are not predicted for compound **1**. These binding modes allowed the formation of hydrogen bonds with the backbones of R50 and I108 and with the phosphate group of the substrate; of electrostatic interactions with the side chains of D49, N112, D218, R175′, and the 3′-hydroxyl group of the ribose moiety of dUMP; and of van del Waals interactions with 10 other residues, including M311 and A312. Compound **1** shows similar, but not identical, binding modes. In fact, it was not able to assume these same binding modes because of clashes with M311 and A312.

Other differences are in regard to secondary binding modes near the small domain region. Both compounds interact with R50, R176′, and dUMP; however, while compound **1** also forms hydrogen bonds with D49, S120, A191, and Y258, compound **2** hydrogen-bonds to M190 and R175′.

Profiling Bacterial Strain Inhibition

A subset of molecules (**5**, **8**, **10**, **13**−**16**, and **18**) was selected and tested against a collection of 18 Gram-positive or Gram-negative bacterial strains. The compounds were selected mainly on the basis of their enzyme inhibition profile and solubility. The minimum inhibitory concentrations (MIC), defined as the lowest concentration at which bacterial growth is no longer evident, were ascertained. The MIC values of the substances are listed in Table 3 and compared to ciprofloxacin (cpx), a member of the fluorquinolone family with a broad spectrum of action. The active compounds **5**, **10**, and **13**−**16** showed a limited spectrum of action, being active mainly toward Gram-positive bacteria. The MIC values were often similar to that of cpx, in the range 0.5−12.5 μg/mL.

The MTT test was performed to evaluate the toxicity of compounds **5**, **10**, and **14**−**16** against VERO cell cultures. The data in Table 4 clearly show the absence of toxicity, especially for **5** and **15**. Cell growth was not significantly modified by the presence of different concentrations of the other compounds. Three compounds (**5**, **10**, and **15**) were also tested against 23 clinical isolate multiresistant bacterial strains recovered from hospitalized patients who have been treated with different antibiotics, such as β-lactam, macrolides, and aminoglycosidic. The measured MIC values ranged between 2.5 and 0.5 μg/mL (Table 5). The most interesting results are related to compounds **5** and **15**, showing a MIC value of 0.5 μg/mL against *Staphylococcus epidermidis* 35, a strain that is resistant to 17 antibiotics. No activity is evident for compound **10** against the multiresistant strains (Table 5).

Figure 5 shows the growth curve recorded biophotometrically over 24 h of *Staphylococcus epidermidis* alone (control) and in

Table 4. Results of MTT Test on VERO Cells[a]

	compd					
concn (mg/L)	control	**5**	**10**	**15**	**16**	**14**
50	100	> 100	58	80	61	41
25	100	100	70	>100	85	84
12.05	100	100	90	>100	97	100
6.25	100	100	90	>100	97	100
3.12	100	100	90	>100	95	100
1.56	100	100	90	>100	96	100

[a] Data are expressed as percentage of cellular growth. Control vessels are without compounds.

Table 5. MIC Values (μg/mL) of Compouds **5**, **10**, and **15** Tested against 23 Multiresistant Bacterial Strains

	compd		
strains	**5**	**10**	**15**
Staphylococcus epidermidis 45	1	2.5	>65
Staphylococcus epidermidis 39	1	2.5	>65
Staphylococcus epidermidis 42	2.5	5	>65
Staphylococcus epidermidis 33	1	2.5	>65
Staphylococcus epidermidis 35	0.5	0.5	>65
Staphylococcus epidermidis 30	1	5	>65
Staphylococcus epidermidis 32	1	2.5	>65
Staphylococcus epidermidis 50	1	2.5	>65
Staphylococcus epidermidis 21	2.5	5	>65
Staphylococcus epidermidis 48	1	2.5	>65
Staphylococcus epidermidis 36	1	2.5	>65
Staphylococcus aureus 27	2.5	5	>65
Staphylococcus aureus 15	2.5	10	>65
Staphylococcus aureus 9	5	10	>65
Staphylococcus aureus 17	2.5	5	>65
Staphylococcus haemolyticus 51	5	5	>65
Staphylococcus haemolyticus 56	5	10	>65
Enterococcus faecium 52	5	10	>65
Enterococcus faecium 28	>100	>75	>65
Enterococcus faecium 57	5	10	>65
Enterococcus faecium 6	5	10	>65
Enterococcus gallinarum 37	2.5	10	>65
Enterococcus gallinarum 64	1	2.5	>65

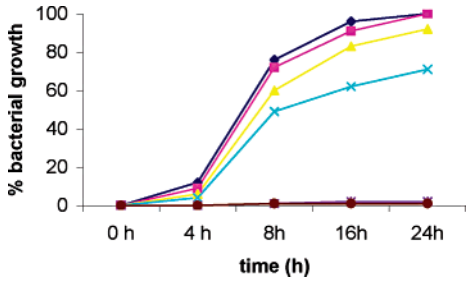

Figure 5. Growth curves of *Staphylococcus epidermidis*, clinical isolate, in the presence of compound **5**: (blue) control; (pink) 0.1 μg/mL; (yellow) 0.5 μg/mL; (light-blue) 1 μg/mL; (violet) 5 μg/mL; (brown) 25 μg/mL.

the presence of different concentrations of compound **5**. At 0.1 μg/mL no effect on *Staphylococcus epidermidis* growth was observed. By contrast, antibacterial activity was evident after 8 h at a dose of 0.5 μg/mL. The best results were obtained with 1.0 μg/mL (corresponding to the MIC value for most of the strains). The remaining dosages had a bactericidal effect.

Discussion

New 1,2-naphthalein derivatives have been designed and synthesized. All the compounds and a few more previously reported 1,8-naphthaleins were tested against a TS-based biolibrary mostly from pathogen TS enzymes, in addition to hTS and hDHFR. In the 1,2-naphthalein series the most species-specific was compound **1** (K_i against CnTS of 0.4 μM and SI $K_{i\ hTS}/K_{i\ CnTS}$ of 330 with respect to hTS). By contrast, compound **2** was very active against both pathogen and human TS (K_i for the latter of 0.4 μM). In the 1,8-naphthalein series, compounds **10** and **11** were the most active against LcTS (K_i of 0.7 μM), while compound **16** was the most species-specific (SI of 306, with respect to this enzyme). The most species-specific compounds, of great interest as leading antibacterial agents, were **5**, **10**, **13**−**16**, and **18**. The K_i values ranged from 0.7 to 1.7 as the best result for each compound considered. The SI $K_{i\ hTS}/K_{i\ LcTS}$ determined so far ranged from 50 to 330.

Out of all the derivatives, **17** was the most species-specific (SI $K_{i\ hTS}/K_{i\ EcTS} = 365$).

The selected species-specific compounds were considered for further in vitro studies against bacterial wild-type and clinical isolates.

The data referring to the 1,2-naphthalein series suggest a relationship between the structural isomeric form and the observed specificity. In fact, only β-isomer **2** showed affinity for both pathogen and human enzymes while the α-isomers were all inactive (**1**, **3**−**5**, **8**) or poorly active (**7**) toward the latter.

With the aim of understanding the observed enzyme inhibition profile, molecular modeling studies were performed and the AutoDock 3.0.5 program was applied to calculate the most favorable binding site of compounds **1** and **2** toward LcTS and hTS. The results suggested that these molecules could bind in both enzymes in two regions, in the folate-binding site and near the small domain region. As already observed in the case of other naphthalein derivatives and in agreement with experimental data derived from site-directed mutagenesis and enzyme kinetic studies,[14] for compounds **1** and **2** the AutoDock results suggest a multiple binding mode that is typical of the phthalein structure.[14,17] The results highlight some differences in the binding modes of compounds **1** and **2** in the hTS active site. In particular, compound **2** seems to be able to take advantage of the favorable interactions with F80, M311, and A312.

On the basis of the biolibrary screening results, eight compounds were selected for multistep cell-based assays. The first screening was done on 18 wild-type bacterial cell lines, including Gram-positive and Gram-negative bacteria, such as *Enterobacter*, *Staphylococcus*, and *Escherichia*. Of eight molecules, the five most interesting compounds were tested using MTT tests to evaluate their cytotoxicity. Compounds **5**, **15**, and **10** showed null or very low toxicity in the assay, suggesting that these molecules could be selected for further experiments. Then a second level of cell-based assays was performed against clinical isolate resistant strains. Different clinical specimens (blood and purulent exudates) from the microbiology laboratory of Modena Hospital were processed for cultural analysis.[19] Particular attention was paid to the *Enterococcus* strains with full or medium sensitivity to teicoplanin and vancomycin. Two of them were fully resistant and one was medium-resistant to vancomycin. Among the *Staphylococcus* strains, 13 showed medium resistance to teicoplanin, 10 of them belonged to the species *Staphylococcus epidermidis*, while another belonged to *Staphylococcus aureus* and the other two to *Staphylococcus haemoliticus*. *Staphylococcus* and *Enterococcus* are among the Gram-positive that are most frequently involved in infective processes.

In our study, compounds **5** and **15** showed good activity against most of the multiresistant strains tested, in particular against *Staphylococcus epidermidis*. In contrast, the previously reported compound **10** was completely ineffective against the resistant strains, even if it was effective against wild-type Gram-positive bacteria (Table 5).

Compound **5** was tested against all the above-described multiresistant strains, and the best result was obtained against *Staphylococcus epidermidis* 35 (Figure 5), showing an MIC value of approximately 0.5 μg/mL.

Conclusions

We have previously synthesized and tested a series of 1,8-naphthalein analogues, which showed interesting biological activity profiles against model bacterial cell lines from ATCC and low toxicity vs human cells. The best inhibitors showed a K_i of 0.5 μM and a MIC of 1.8 μg/mL. In the present paper we obtained a compound (**5**) showing 2 times better efficacy against clinical isolates bacterial cells. The K_i value was in the same order as those of the previous naphthaleins; thus, we successfully improved the cellular pharmacokinetic profile. The clinical isolates showed drug resistance vs a number of antibiotics and chemotherapeutic agents including vancomycin, an antibiotic indicated for the treatment of serious, life-threatening infections by Gram-positive bacteria, which are unresponsive to other less toxic antibiotics. Compound **5** is suggested as a possible lead with promising antibacterial activity.

The chemistry of 1,2-naphthalein derivatives allowed an easier derivatization of the core skeleton from the perspective of further functionalization with respect to 1,8-naphthalein analogues.

As an important remark, we observe that an interpretation of the specificity profile of the two compounds **1** and **2** against LcTS and hTS enzymes is accessible through modeling studies. The parallel behavior of the biological profile against bacterial cell lines does not lead to the conclusion that thymidylate synthase enzymes are the exclusive intracellular target of the identified leads. More pharmacology studies are needed for this conclusion.

The results presented confirm the relevance of the naphthalein derivatives as antinfective agents and are encouraging further developments to clarify their full mechanism of action.

Experimental Section

Chemistry. The melting points were determined using Büchi 510 capillary melting point apparatus and are uncorrected. The elemental analyses for the test compounds were within ±0.4 of the theoretical values. TLC on silica gel plates was used to check product purity. Silica gel 60 (Merck, 230−400 mesh) was used for flash chromatography. The structures of all the compounds were consistent with their analytical and spectroscopic data. NMR spectra were performed on a Bruker FT-NMR AVANCE400.

NMR data of compounds **1**−**8**, **16**, **18** are reported in Table 6.

Synthesis of 1,1-Bis(4-hydroxyphenyl)-1*H*-naphtho[1,2-*c*]furan-3-one (1) and 3,3-Bis(4-hydroxyphenyl)-3*H*-naphtho[1,2-*c*]furan-1-one (2). The compounds were obtained by condensing the 1,2-naphthalic anhydride and phenol according to a known procedure.[20] Separation was accomplished by flash chromatography, eluting with dichloromethane/methanol, 98/2. For **1**, the yield was 15%. For **2**, the yield was 1%. Anal. ($C_{24}H_{16}O_4$) C, H.

Synthesis of 1,1-Bis(4-hydroxy-3-iodophenyl)-1*H*-naphtho[1,2-*c*]furan-3-one (3). Iodine monochloride (0.65 mmol) in glacial acetic acid (1 mL) was added dropwise to a mixture of **1** (0.05 g, 0.14 mmol) suspended in glacial acetic acid (2.5 mL), and the mixture was stirred overnight at room temperature. After evaporation of the solvent, the residue was purified by flash chromatography, eluting with dichloromethane/methanol, 98/2, to give 0.062 g of **3** (71.2%). Anal. ($C_{24}H_{14}I_2O_4$) C, H, I.

Synthesis of 1,1-Bis(3-bromo-4-hydroxyphenyl)-1*H*-naphtho[1,2-*c*]furan-3-one (4). A solution of bromine (0.27 mmol) in dichloromethane (1 mL) was added dropwise to a solution of **1** (0.05 g, 0.14 mmol) in dichloromethane (3 mL), under stirring at room temperature. After 5 h the solvent was evaporated and the residue purified by flash chromatography, eluting with dichloromethane/methanol, 98/2, to give **4** (28%). Anal. ($C_{24}H_{14}Br_2O_4$) C, H, Br.

Synthesis of 1,1-Bis(3,5-dibromo-4-hydroxyphenyl)-1*H*-naphtho[1,2-*c*]furan-3-one (5). Excess bromine (0.7 mL) was added dropwise at room temperature to a solution of **1** (0.05 g, 0.14 mmol) in ethanol (2 mL), and the mixture was stirred overnight. The solvent was evaporated and the residue purified by flash chromatography, eluting with cyclohexane/ethyl acetate, 80/20, to give **5** (64.5%). Anal. ($C_{24}H_{12}Br_4O_4$) C, H, Br.

Synthesis of 1,1-Bis(4-hydroxy-5-isopropyl-2-methylphenyl)-1*H*-naphtho[1,2-*c*]furan-3-one (6). Aluminum chloride (0.67 g, 5 mmol) was added portionwise to a mixture of 1,2-naphthalic anhydride (0.5 g, 2.5 mmol) and thymol (5 mmol) in *s*-tetrachloroethane (25 mL), and the mixture was stirred at 115 °C for 3 days. The still hot mixture was poured onto ice and dichloromethane was added. After stirring for 0.5 h, the insoluble was filtered off. The organic layer was separated, dried over sodium sulfate, and concentrated under vacuum. The residue was purified by flash chromatography, eluting with cyclohexane/ethyl acetate, 70/30, to give 0.07 g of **6** (5.8%). Anal. ($C_{32}H_{32}O_4$) C, H.

Synthesis of 3,3-Bis(3-chloro-4-hydroxyphenyl)-3*H*-naphtho[1,2-*c*]furan-1-one (7) and 3,3-Bis(3-fluoro-4-hydroxyphenyl)-3*H*-naphtho[1,2-*c*]furan-1-one (8). A mixture of 1,2-naphthalic anhydride (0.5 g, 2.5 mmol), the appropriate phenol (5.0 mmol), and a few drops of sulfuric acid was heated under stirring at 180 °C for 5 h. After the mixture was cooled, water was added and the mixture was extracted with dichloromethane (3 × 30 mL). The organic layer was dried over sodium sulfate, and the solvent was evaporated. The residue was purified by flash chromatography, eluting with dichloromethane/methanol, 95/5. For **7**: 0.085 g (7.8%). Anal. ($C_{24}H_{14}Cl_2O_4$). For **8**: 0.068 g (6.8%). Anal. ($C_{24}H_{14}F_2O_4$) C, H, F.

Synthesis of 1,8-Naphthaleins. 6(7)-Chloro-3,3-bis(3-bromo-4-hydroxyphenyl)-1*H*,3*H*-naphtho[1,8-*c*,*d*]pyran-1-one (16). Bromine (7.5×10^{-3} mL, 0.146 mmol) in 0.5 mL of dichloromethane was added dropwise, under stirring, to a solution of 6-chloro-3,3-bis(4-hydroxyphenyl)-1*H*,3*H*-naphtho[1,8-*c*,*d*]pyran-1-one[13] (0.03 g, 0.07 mmol) in 2 mL of dichloromethane. The reaction mixture was stirred at room temperature for 4 h. After evaporation of the solvent, the residue was purified by flash chromatography, eluting with dichloromethane/methanol, 98/2, to give 0.004 g of **16** (10.2%). Anal. ($C_{24}H_{13}Br_2ClO_4$) C, H, Br, Cl.

6(7)-Chloro-3,3-bis(3-fluoro-4-hydroxyphenyl)-1*H*,3*H*-naphtho[1,8-*c*,*d*]pyran-1-one (18). To a mixture of the commercially available 4-chloro-1,8-naphthalic anhydride (0.5 g, 2.15 mmol) and 2-fluorophenol (0.383 mL, 4.3 mmol) 5 drops of H_2SO_4 were added. The mixture was left under stirring at 180 °C for 5 h. After the mixture was cooled, the residue was purified by flash chromatography, eluting with dichloromethane/methanol (98/2) to give 0.02 g of **18** (2.12%). Anal. ($C_{24}H_{13}ClF_2O_4$) C, H, Cl, F.

It is noted that because of the presence of a chlorine atom on the naphthalene ring, in the cases of both **16** and **18**, a mixture of 6 or 7 substituted isomers was obtained, which was tested as such.

Biological Evaluation. Purification of the Enzymes. All the strains and plasmids were provided by Dr. D. V. Santi, from the University of California, San Francisco. The expression and purification of LcTS, EcTS, CnTS, and hTS were done following known procedures.[21−24] The enzyme LcTS was purified by column chromatography using phosphocellulose (P11, Biorad) and hydroxyapatite (HAP, Biorad) resin, using phosphate buffer as the eluent. EcTS, CnTS, and hTS were purified as previously reported.[13] The enzyme preparations were >95% homogeneous as visualized by SDS (sodium dodecyl sulfate) polyacrylamide gel electrophoresis. The purified enzymes were stored at −80 °C in 10 mM phosphate buffer, pH 7.0, and 0.1 mM EDTA. The enzyme activity was determined spectrophotometrically by steady-state kinetic analysis, following the increasing absorbance at 340 nm due to the oxidation reaction of N^5,N^{10}-methylenetetrahydrofolate (mTHF) to dihydrofolate (DHF).[25] An amount of 1 mL of reaction solution was formed by standard assay buffer, pH 7.4, dUMP (100 μM), 6(*R*,*S*)-1-CH_2CH_4-folate (140 μM) (Sigma), and enzyme (0.07 μM). Assays were performed at 20 °C in the standard assay buffer formed by TES (*N*-tris(hydroxymethyl)methyl-2-aminoethanesulfonic acid) (50 mM) at pH 7.4, $MgCl_2$ (25 mM), formaldehyde (6.5 mM), EDTA (1 mM), and 2-mercaptoethanol (75 mM). hDHFR (DHFR, E.C. 1.5.1.3) was purified through alternate steps of column chromatography and ammonium sulfate precipitations as reported.[26] DHFR catalyzes the NADPH-dependent reduction of dihydrofolate (DHF) to tetrahydrofolate (THF). The assays were run spectrophotometrically by measuring the decrease in absorbance at 340 nm upon DHF reduction at 25 °C. One enzyme unit is defined as 1 nmol of DHF reduced per minute. The reaction mixture was formed by 50 μM TES, pH 7.0, 1 μM EDTA, 75 μM 1-mercaptoethanol, 100 μM NADPH, and 58.03 μM DHF.[27]

Assays. Stock solutions of the inhibitors were prepared in DMSO (dimethyl sulfoxide) and stored at −20 °C until use. Compound **4** was tested as a racemic mixture. The inhibition pattern for all the compounds was determined by steady-state kinetic analysis of the dependence of enzyme activity on folate concentration at varying inhibitor concentrations. All the compounds showed competitive inhibition. K_i values were obtained from the linear least-squares fit of the residual activity as a function of inhibitor concentration, using suitable equations for competitive inhibition.[28] Each experiment was repeated at least three times, and no individual measurement differed by more than 20% from the mean. The maximum solubility is reported when a molecule does not show any inhibition of TS activity at the solubility limit. To better understand the biological activity profile, we simulated the IC_{50} values assuming an inhibition of 2% at the solubility limit and calculating a projected IC_{50} for the compounds studied.[9,17] This number underestimates the potency of the inhibition, but it is helpful in the comparative analysis of the specificity index (SI),[9] which was determined by the ratio $K_{i\ hTS}/K_{i\ other\ enzyme}$. SSI was determined by the ratio $K_{i\ hTS}/K_{i\ hDHFR}$.

The effect of increasing DMSO concentration in the TS assay mixture was studied, and it was observed that no change in TS activity was seen at concentrations up to 8% DMSO.[29]

Microbiology. A collection of 18 Gram-positive and Gram-negative wild-type bacterial strains were tested against the selected molecules (Table 3).

Table 6. NMR Data (δ, ppm) of Compounds **1**−**8**, **16**, **18**

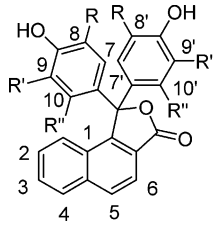

1, 3, 4, 5, 6

	1	3	4	5	6		1	3	4	5	6
1	7.94 d	7.97 d	7.96 d	8.12 d	7.70 d	14					1.10 t
2	7.69 t	7.77 t	7.74 t	7.75 t	7.58 t	15					=H15
3	7.84 t	7.88 t	7.87 t	7.84 t	7.80 t	6′					
4	8.30 d	8.34 d	8.32 d	8.28 d	8.30 d	7′	=H7	=H7	7.60 d J_m	=H7	6.60 d J_m
5	8.35 d	8.40 d	8.38 d	8.34 d	8.35 d	8′	=H8				
6	8.05 d	8.08 d	8.07 d	8.14 d	8.00 d	9′	=H9	=H9	7.32 over.		6.90 d J_m
7	7.31 d J_o	7.54 d J_m	7.00 d J_o	7.79 s	7.05 d J_m	10′	=H10	=H10	7.15 d J_o	=H7	
8	6.99 d J_o					11′					9.55 s
9	=H8	7.20 d J_o	=H8		6.53, d J_m	12′					2.22 s
10	=H7	7.37 dd J_o-J_m	=H7	=H7		13′					3.05 m
11					9.50 s	14′					0.65 t
12					1.72 s	15′					0.77 t
13					3.22 m						

1. COSY: H1−H2; H2−Hl3; H3−H4; H5−H6; H7−H8. NOE: H4−H5; H1−H7. Solvent: acetone-d_6. Temp = 25 °C.
3. COSY: H1−H2,H3; H2−H3; H4−H3,H2; H5−H6; H9−H10; H7−H10. NOE: H4−H5; H1−H2,H7,H10. Solvent: acetone-d_6. Temp = 25 °C.
4. COSY: H1−H2,H3; H2−H3; H4−H3,H2; H5−H6; H7′−H10′; H9′−H10′; NOE: H4−H5; H1−H7. Solvent: acetone-d_6. Temp = 25 °C.
5. COSY: H1−H2; H2−H3; H3−H4; H5−H6. Solvent: acetone-d_6 + benzene-d_6. Temp = 25 °C.
6. COSY: H1−H2; H2−H3; H3−H4; H5−H6; H7−H8. NOE: H4−H5; H1−H7. Solvent: acetone-d_6. Temp = 25 °C.

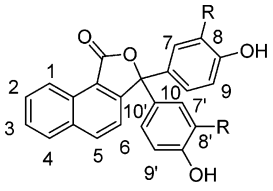

2, 7, 8

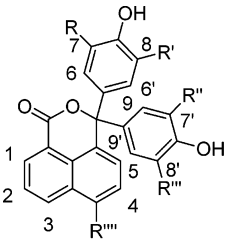

16, 18

	2	7	8		16	18
1	7.95 d	9.14 d	9.14 d	1	8.51 d	8.49 d
2	7.69 t	7.95 t	7.97 t	2	8.03 t	8.01 t
3	7.41 t	7.85 t	7.87 t	3	8.68 d	8.65 d
4	8.30 d	8.26 d	8.29 d	4	7.95 d	7.93 d
5	8.35 d	8.50 d	8.52 d	5	7.20 d	7.17 d
6	8.05 t	8.02 d	8.02 d	6	7.28 d J_m	7.20 dd $^3J_{HF}$−J_m
7	7.31 d	7.54 d J_m	7.29 dd $^3J_{HF}$−J_m	7		
8	6.99 d			8	7.03 d J_o	7.05 t J_o
9	=H8	7.20 d J_o	7.17 dd $^4J_{HF}$−J_o	9	6.97 dd J_o−J_m	7.10 dd J_o−J_m
10	=H7	7.37 dd J_o−J_m	7.22 dd J_o−J_m	6′	=H6	=H6
7′	=H7	=H7	=H7	7′		
8′	=H8			8′	=H8	=H8
9′	=H9	=H9	=H9	9′	=H9	=H9
10′	=H10	=H10	=H10			

16. COSY: H1−H2; H2−H3; H4−H5; H6−H9; H8−H9; H6′−H9′; H8′−H9′. Solvent: DMSO-d_6. Temp = 25 °C.
18. COSY: H1−H2; H2−H3; H4−H5; H6−H9; H8−H9; H6′−H9′; H8′−H9′, Solvent: DMSO-d_6. Temp = 25°C.

2. COSY: H1−H2, H2−H3; H3−H4, H5−H6; H7−H9; H7−H12; H9−H12; H14,15−H13; H7′−H9′; H7′−H12′; H9′−H12′; H14′−H13′; H15′−H13′. NOE: H1−H7; H9−H11; H7−H14,H15; H1−H7′; H9′−H11′; H7′−H14′; H7′−H15′. Solvent: DMSO-d_6. Temp = 25 °C.
7. COSY: H1−H2; H2−H3; H3−H4; H5−H6; H9−H10; H7−H10. NOE: H4−H5; H6−H10; H6−H7. Solvent: acetone-d_6. Temp = 25 °C.
8. COSY: H1−H2; H2−H3; H3−H4; H5−H6; H9−H10; H7−H10. NOE: H4−H5. Solvent: acetone-d_6. Temp = 25 °C.

Twenty-three strains, comprising strains of *Staphylococcus epidermidis* (11 strains), *Staphylococcus aureus* (4 strains), *Staphylococcus haemoliticus* (2 strains), *Enterococcus faecium* (4 strains), and *Enterococcus gallinarum* (2 strains), were tested. All the strains showed multidrug resistance and were clinical isolates recovered from blood or urine of patients without malignancies. The strains were resistant to at least 17 of the most used antibacterial agents including vancomycin[19,30−36] (Supporting Information).

Sensitivity Test. The Gram-positive and Gram-negative bacteria were cultured in a Mueller−Hinton broth (Difco Milan, Italy) at 37 °C for 24 h. While the bacteria were developing exponentially, they were diluted in a liquid sterile medium to obtain a final innoculum of approximately 1×10^4 CFU/mL and subsequently put in contact with increasing concentrations of the compounds under study. The minimum inhibitory concentrations (MICs), defined as the lowest concentration at which bacterial growth was no longer evident, were ascertained.

Cytotoxicity Test. The Trypan blue exclusion and MTT tests were performed using VERO cells cultured in MEM medium supplemented with 5% heat-inactivated (56 °C, 30 min) fetal calf serum (FCS), 1% of penicillin (50 U/mL), streptomycin (50 μg/mL), and L-glutamine (1%), according to the method described by Ishioka.[37] The cultures were observed for 2 days under the microscope with indirect light. Afterward, a count of living cells was performed. Subsequently, increasing concentrations of the substances were put in contact with the cultures of VERO cells. A vessel in which only cells were present was assumed as a control. After 24 h of incubation, the measurement of active mitochondrial dehydrogenases of living cells (MTT test) was performed.[38]

Molecular Docking. The program AutoDock 3.0.5[39] was used for the docking of compounds **1** and **2**. Since multiple three-dimensional structures of LcTS were available in the PDB,[40] two different conformations of LcTS (1TSL, 1TSM)[14] were considered, together with a modeled open conformation of hTS.[15] Ligands and water molecules were removed from the active site. A molecule of dUMP was added instead and considered part of the target for docking. The structure and coordinates of the dUMP molecule were taken from the ternary complex structures of LcTS (1LCA)[41] and hTS (1I00),[42] respectively, after matching, on the basis of protein trace atoms, these structures to those used for the AutoDock calculations. The same starting complexes (1TSL + dUMP, hTS + dUMP) were already used in another published work.[15] To run AutoDock, dimeric protein structures were prepared with InsightII.[43] Polar hydrogen atoms were added using the WHATIF program.[44] Solvation parameters and atomic partial charges were assigned to the protein using the programs q.kollua and addsol, which are included in the AutoDock program suite. For dUMP, the solvation parameters and atom partial charges were manually added on the basis of the atoms' similarity to protein atoms and of literature data, respectively.[45] Compounds **1** and **2** were built using InsightII. Their geometries were optimized using the program Amsol 6.6 (AM1).[46] The atomic partial charges were calculated using the program RESP (Amber 6.0),[47] on the basis of electrostatic potentials generated by Gaussian 98 (HF/6-31G* as basis set).[48] The program Babel[49] was used to prepare the input **Z** matrix of Amsol and Gaussian. A cubic grid with 22.5 Å long sides, centered on the TS active site, was defined in the case of hTS, whereas cubic grids with 20.6 and 30.4 Å long sides were used with 1TSL and 1TSM, respectively. These grids were wide enough to comprise all of the enzymatic active sites. A Lamarckian genetic algorithm was used to generate 50 bound conformations for compounds **1** and **2** in each protein studied. All nonterminal rotable bonds were allowed to rotate during the calculation. All other settings were kept as default. The results were visually analyzed using the InsightII program. The results of the calculations performed on the two conformations of LcTS were considered altogether. On the basis of the clustering histogram output from the AutoDock program, the lowest energy conformation of each cluster was selected. The selected conformations were grouped on the basis of their binding sites. Two main binding sites were considered, the folate and the crystallographic binding site of compound **10**.[14,15] For each binding site, multiple binding modes were considered. All the conformations that were outside the active site were disregarded.

Acknowledgment. This work was supported by MIUR Cofin 2004 (Grant Costi 2004030405_004) and FIRST 2004. We thank Dr. D. V. Santi (University of California, San Francisco) for giving us plasmids and strains for hTS, CnTS, EcTS, and LcTS

Supporting Information Available: Multidrug resistance data of clinical isolates multidrug-resistant strains used and elemental analysis results of the synthesized compounds. This material is available free of charge via the Internet at http://pubs.acs.org.

References

(1) Carreras, C. W.; Santi, D. V. The catalytic mechanism and structure of thymidylate synthase. *Annu. Rev. Biochem.* **1995**, *64*, 721−762.
(2) Chu, E.; Callender, M. A.; Farrell, M. P.; Schmitz, J. C. Thymidylate synthase inhibitors as anticancer agents: from bench to bedside. *Cancer Chemother. Pharmacol.* **2003**, *52* (Suppl. 1), S80−S89.
(3) Liu, J.; Schmitz, J. C.; Lin, X.; Tai, N.; Yan, W.; Farrell, M.; Bailly, M.; Chen, T.; Chu, E. Thymidylate synthase as a translational regulator of cellular gene expression. *Biochim. Biophys. Acta* **2002**, *1587*, 174−182.
(4) Chu, E.; Allegra, C. J. The role of thymidylate synthase as an RNA binding protein. *BioEssays* **1996**, *18*, 191−198.
(5) Bruni, P.; Minopoli, G.; Brancaccio, T.; Napolitano, M.; Faraonio, R.; Zambrano, N.; Hansen, U.; Russo, T. Fe65, a ligand of the Alzheimer's beta-amyloid precursor protein, blocks cell cycle progression by down-regulating thymidylate synthase expression. *J. Biol. Chem.* **2002**, *277* (38), 35481−35488.
(6) Costi, M. P.; Ferrari, S.; Venturelli, A.; Calò, S.; Tondi, D.; Barlocco, D. Thymidylate synthase structure, function and implication in drug discovery. *Curr. Med. Chem.* **2005**, *12* (19), 2241−2258.
(7) Tondi, D.; Venturelli, A.; Ferrari, S.; Ghelli, S.; Costi, M. P. Improving specificity vs bacterial thymidylate synthases through *N*-dansyl modulation of didansyltyrosine. *J. Med. Chem.* **2005**, *48*, 913−916.
(8) Calò, S.; Tondi, D.; Venturelli, A.; Ferrari, S.; Pecorari, P.; Rinaldi, M.; Ghelli, S.; Costi, M. P. A step further in the discovery of phthalein derivatives as thymidylate synthase inhibitors. *ARKIVOC* **2004**, 382−396.
(9) Ghelli, S.; Rinaldi, M.; Barlocco, D.; Gelain, A.; Pecorari, P.; Tondi, D.; Rastelli, G.; Costi, M. P. Ortho-halogen naphthaleins as specific inhibitors of *Lactobacillus casei* thymidylate synthase. Conformational properties and biological activity. *Bioorg. Med. Chem.* **2003**, *11*, 951−963.
(10) Costi, M. P.; Tondi, D.; Rinaldi, M.; Barlocco, D.; Pecorari, P.; Soragni, F.; Venturelli, A.; Stroud, R. M. Structure-based studies on species-specific inhibition of thymidylate synthase. *Biochim. Biophys. Acta* **2002**, *1587*, 206−214.
(11) Fritz, T. A.; Tondi, D.; Finer-Moore, J. S.; Costi, M. P.; Stroud, R. M. Predicting and harnessing protein flexibility in the design of species-specific inhibitors of thymidylate synthase. *Chem. Biol.* **2001**, *8*, 981−995.
(12) Tondi, D.; Slomczynska, U.; Costi, M. P.; Watterson, D. M.; Ghelli, S.; Shoichet, B. K. Structure-based discovery and in-parallel optimization of novel competitive inhibitors of thymidylate synthase. *Chem. Biol.* **1999**, *6*, 319−331.
(13) Costi, M. P.; Rinaldi, M.; Tondi, D.; Pecorari, P.; Barlocco, D.; Ghelli, S.; Stroud, R. M.; Santi, D. V.; Stout, T. J.; Musiu, C.; Marangiu, E. M.; Pani, A.; Congiu, D.; Loi, G. A.; La Colla, P. Phthalein derivatives as a new tool for selectivity in thymidylate synthase inhibition. *J. Med. Chem.* **1999**, *42*, 2112−2124.
(14) Stout, T. J.; Tondi, D.; Rinaldi, M.; Barlocco, D.; Pecorari, P.; Santi, D. V.; Kuntz, I. D.; Stroud, R. M.; Shoichet, B. K.; Costi, M. P. Structure-based design of inhibitors specific for bacterial thymidylate synthase. *Biochemistry* **1999**, *38*, 1607−1617.
(15) Ferrari, S.; Costi, M. P.; Wade, R. Inhibitor specificity via protein dynamics: insights from the design of antibacterial agents targeted against thymidylate synthase. *Chem. Biol.* **2003**, *10*, 1183−1193.
(16) Hardy, L. W.; Finer-Moore, J. S.; Montfort, W. R.; Jones, M. O.; Santi, D. V.; Stroud, R. M. Atomic structure of thymidylate synthase: target for rational drug design. *Science* **1987**, *235*, 448−455.
(17) Shoichet, B. K.; Stroud, R. M.; Santi, D. V.; Kuntz, I. D.; Perry, K. M. Structure-based discovery of inhibitors of thymidylate synthase. *Science* **1993**, *259*, 1445−1450.
(18) Hershberg, E. B.; Fieser, L. F. 3,4-Dihydro-1,2-naphthalic anhydride. *Org. Synth., Collect. Vol.* **1969**, *II*, 194−196, 423−424.
(19) Murray, P. R.; Baron, E. J.; Pfaller, M. A.; Tenover, F. C.; Yolken, R. H. *Manual of Clinical Microbiology*, 7th ed.; AMS Press: Washington, DC, 1999.
(20) Hubacher, M. H. The phthaleins from phenol and 1,2-naphthalenedicarboxylic acid. *J. Am. Chem, Soc.* **1944**, *66*, 255−256.
(21) Kealey, J. T.; Santi, D. V. Purification methods for recombinant *Lactobacillus casei* thymidylate synthase and mutants: a general, automated procedure. *Protein Expression Purif.* **1992**, *4*, 380−385.
(22) Maley, G. F.; Maley, F. Properties of a defined mutant of *Escherichia coli* thymidylate synthase. *J. Biol. Chem.* **1988**, *263*, 7620−7627.

(23) Livi, L. L.; Edman, U.; Schneider, G. P.; Greene, P. J.; Santi, D. V. Cloning, expression and characterization of thymidylate synthase from *Cryptococcus neoformans. Gene* **1994**, *150*, 221−226.
(24) Davisson, V.; Sirawaraporn, W.; Santi, D. V. Expression of human thymidylate synthase in *Escherichia coli. J. Biol. Chem.* **1989**, *264*, 9145−9148.
(25) Pogolotti, A. L., Jr.; Danenberg, P. V.; Santi, D. V. Kinetics and mechanism of interaction of 10-propargyl-5,8-dideazafolate with thymidylate synthase. *J. Med. Chem.* **1986**, *29*, 478−482.
(26) Dann, J. G.; Ostler, G.; Bjur, R. A.; King, W. R.; Scudder, P.; Roberts, G. C. K.; Burgen, S. V. Large-scale purification and characterization of dihydrofolate reductase from a methotrexate resistant strain of *Lactobacillus casei. Biochem. J.* **1976**, *157*, 559−571.
(27) Meek, T. D.; Garvey, E. P.; Santi, D. V. Purification and characterization of bifunctional thymidylate synthetase-dihydrofolate reductase from methotrexate-resistant *Leismania tropicae. Biochemistry* **1985**, *24*, 678−686.
(28) Segel, I. H. *Enzyme Kinetics. Behaviour and Analysis of Rapid Equilibrium and Steady-State Enzyme Systems*; John Wiley and Sons: New York, 1975; p 105.
(29) Soragni, F.; Costi, M. P. Unpublished data.
(30) Centers for Disease Control and Prevention. *Staphylococcus aureus* resistant to vancomycin. United States. *MMWR Morbid. Mortal. Wkly Rep.* **2002**, *51* (26), 565−567.
(31) Tabaqchali, S. Vancomycin-resistant *Staphylococcus aureus*: apocalypse now? *Lancet* **1997**, *350*, 1644−1645.
(32) Noble, W. C.; Virani, Z.; Cree, R. G. A. Co-transfer of vancomycin and other resistance genes from *Enterococcus faecalis* NCTC 12201 to *Staphylococcus aureus. FEMS Microbiol. Lett.* **1992**, *93*, 195−198.
(33) Hiramatsu, K.; Hanak, H.; Ino, T.; Yabuta, K.; Oguri, T.; Tenover, F. C. Methicillin-resistant *Staphylococcus aureus* clinical strain with reduced vancomycin susceptibility. *J. Antimicrob. Chemother.* **1997**, *40*, 135−136.
(34) Mainardi, J. l.; Shalaes, D. M.; Goering, J. H.; Shalaes, J. H.; Acar, J. F.; Goldtein, F. W. Decreased teicoplanin susceptibility of methicillin-resistant strains of *Staphylococcus aureus. J. Infect. Dis.* **1995**, *171*, 1646−1650.
(35) Diekema, D. J.; Pfaller, M. A.; Jones, R. N. The SENTRY Participants Group. Age-related trends in pathogen frequency and antimicrobial susceptibility of bloodstream isolates in North America. SENTRY Antimicrobial Surveillance Program, 1997−2000. *Int. J. Antimicrob.* **2002**, *20*, 412−418.
(36) Stinear, T. P.; Olden, D. C.; Johnson, P. D. R.; Davies, J. K.; Gryson, M. L. Enterococcal vanB resistance locus in anaerobic bacteria in human faeces. *Lancet* **2001**, *357*, 855−856.
(37) Ishioka, C.; Kanamaru, R.; Sato, T.; Dei, T.; Konishi, Y.; Asamura, M.; Wakui, A. Inhibitory effects of prostaglandin A2 on c-myc expression and cell cycle progression in human leukemia cell line HL-60. *Cancer Res.* **1988**, *48*, 2813−2818.
(38) Mosman, T. Rapid colorimetric assay for cellular growth and survival: application to proliferation and cytotoxicity assays. *J. Immunol. Methods* **1983**, *65*, 55−63.
(39) Morris, G. M.; Goodsell, D. S.; Halliday, R. S.; Huey, R.; Hart, W. E.; Belew, R. K.; Olson, A. J. Automated docking using a Lamarckian genetic algorithm and an empirical binding free energy function. *J. Comput. Chem.* **1998**, *19*, 1639−1662.
(40) Berman, H. M.; Westbrook, J.; Feng, Z.; Gilliland, G.; Bhat, T. N.; Weissig, H.; Shindyalov, I. N.; Bourne, P. E. The Protein Data Bank. *Nucleic Acids Res.* **2000**, *28*, 235−242.
(41) Finer-Moore, J. S.; Fauman, E. B.; Foster, P. G.; Perry, K. M.; Santi, D. V.; Stroud, R. M. J. Refined structure of substrate-bound and phosphate-bound thymidylate synthase from *Lactobacillus casei. J. Mol. Biol.* **1993**, *232*, 1101−1116.
(42) Almog, R.; Waddling, C. A.; Maley, F.; Maley, G. F.; Van Roey, P. Crystal structure of a deletion mutant of human thymidylate synthase Δ(7−29) and its ternary complex with Tomudex and dUMP. *Protein Sci.* **2001**, *10*, 988−996.
(43) InsightII, Modelling Environment. 2000. http://www.accelrys.com.
(44) Vriend, G. WHATIF: A molecular modelling and drug design program. *J. Mol. Graphics* **1990**, *8*, 52−56.
(45) Cornell, W. D.; Cieplak, P.; Bayly, C. I.; Gould, I. R.; Merz, K. M., Jr.; Ferguson, D. M.; Spellmeyer, D. C.; Fox, T.; Caldwell, J. W.; Kollman, P. A. A second generation force field for the simulation of proteins, nucleic acids, and organic molecules. *J. Am. Chem. Soc.* **1995**, *117*, 5179−5197.
(46) Hawkins, G. D.; Giesen, D. J.; Lynch, G. C.; Chambers, C. C.; Rossi, I.; Storer, J. W.; Li, J.; Winget, P.; Rinaldi, D.; Liotard, D. A.; Cramer, C. J.; Truhlar, D. G. *AMSOL*, version 6.6; University of Minnesota: Minneapolis, MN, 1997.
(47) Case, D. A.; Pearlman, D. A.; Caldwell, J. W.; Cheatham, T. E., III; Ross, W. S.; Simmerling, C. L.; Darden, T. A.; Merz, K. M.; Stanton, R. V.; Cheng, A. L.; Vincent, J. J.; Crowley, M.; Tsui, V.; Radmer, R. J.; Duan, Y.; Pitera, J.; Massova, I.; Seibel, G. L.; Singh, U. C.; Weiner, P. K.; Kollman, P. A. *AMBER 6*; University of California: San Francisco, CA, 1999.
(48) Frisch, M. J.; Trucks, G. W.; Schlegel, H. B.; Scuseria, G. E.; Robb, M. A.; Cheeseman, J. R.; Zakrzewski, V. G.; Montgomery, J. A., Jr.; Stratmann, R. E.; Burant, J. C.; Dapprich, S.; Millam, J. M.; Daniels, A. D.; Kudin, K. N.; Strain, M. C.; Farkas, O.; Tomasi, J.; Barone, V.; Cossi, M.; Cammi, R.; Mennucci, B.; Pomelli, C.; Adamo, C.; Clifford, S.; Ochterski, J.; Petersson, G. A.; Ayala, P. Y.; Cui, Q.; Morokuma, K.; Malick, D. K.; Rabuck, A. D.; Raghavachari, K.; Foresman, J. B.; Cioslowski, J.; Ortiz, J. V.; Stefanov, B. B.; Liu, G.; Liashenko, A.; Piskorz, P.; Komaromi, I.; Gomperts, R.; Martin, R. L.; Fox, D. J.; Keith, T.; Al-Laham, M. A.; Peng, C. Y.; Nanayakkara, A.; Gonzalez, C.; Challacombe, M.; Gill, P. M. W.; Johnson, B. G.; Chen, W.; Wong, M. W.; Andres, J. L.; Head-Gordon, M.; Replogle, E. S.; Pople, J. A. *Gaussian 98*; Gaussian, Inc.: Pittsburgh, PA, 1998.
(49) Walters, P.; Stahl, M. *Babel*, version 1.6; http://smolg.com/chem/babel.

JM051187D